

IN-DEPTH CHARACTERIZATION OF CELLULOSIC PULPS FROM OIL PALM EMPTY FRUIT BUNCHES AND KENAF CORE, DISSOLUTION AND PREPARATION OF CELLULOSE MEMBRANES

SHARIFAH NURUL AIN SYED HASHIM,^{*} BALQIS AZ-ZAHRAA NORIZAN,^{*}
KHAIRUNNISA WAZNAH BAHARIN,^{*} SARANI ZAKARIA,^{*} CHIN HUA CHIA,^{*}
ANTJE POTTHAST,^{**} SONJA SCHIEHSE,^{**} MARKUS BACHER,^{**} THOMAS ROSENAU^{***,**}
and SHARIFAH NABIHAH SYED JAAFAR^{*}

^{*}*Bioresources and Biorefinery Laboratory, Faculty of Science and Technology, Universiti
Kebangsaan Malaysia, 43600 UKM Bangi, Selangor, Malaysia*

^{**}*Division of Chemistry of Renewable Resources, Department of Chemistry, University of Natural
Resources and Life Sciences, Vienna, Muthgasse 18, A-1190 Vienna, Austria*

^{***}*Johan Gadolin Process Chemistry Centre, Åbo Akademi University, Porthansgatan 3,
Åbo/Turku FI-20500, Finland*

✉ *Corresponding author: Sharifah Nabihah Syed Jaafar, nabihah@ukm.edu.my*

Received April 21, 2020

Cellulosic pulps from oil palm empty fruit bunches (EFB) and kenaf core were bleached and characterized with regard to their sugar content, crystallinity, molecular weight, carboxyl group content and solubility in NaOH/urea. The sugar content results showed glucose, mannose and xylose in EFB pulp and only glucose and xylose in the kenaf core cellulosic pulp. The crystallinity indexes of EFB cellulosic pulp and the kenaf core cellulosic pulp were 49 and 51%, respectively. The carboxyl group content of EFB cellulosic pulp was lower than that of kenaf core pulp. However, the molecular weight of EFB cellulose pulp was higher than that of kenaf core pulp. Because the solubility of kenaf core pulp was higher and acceptable, it was successful in forming a cellulose membrane (CM). The CM was cast at two different thicknesses: 0.04 mm and 0.07 mm. CM0.07 had smaller pore sizes, which yielded a higher tensile strength than CM0.04.

Keywords: bleaching, CP-MAS NMR, crystallinity, pore size, SEC-MALLS

INTRODUCTION

Lignocellulosic material is a natural polymer, such as cellulose, hemicellulose and lignin. These materials are renewable, biocompatible and biodegradable. Among these three constituents, cellulose is the most available natural polymer on earth. Cellulose shows great potential for the fabrication of value-added materials, to replace fossil-based materials,¹ due to its natural strength, especially flexural strength. Eventually, the lignin needs to be removed to obtain highly pure cellulose pulp. The delignification process involves pulping and bleaching procedures. The combination of these processes can produce a variety of pulp purity grades, depending on the type of plant used and the pulping/bleaching processes.^{2,3} The potential application and utilization options of the resulting pulps in follow-up processes, *e.g.* papermaking, textiles and membranes, are based on their quality and properties after delignification.

Cellulose is a semi-crystalline and high-molecular-weight polymer. Cellulose has primary hydroxyl groups at C-6 of each anhydroglucose unit (AGU) and secondary hydroxyl groups at C-2 and C-3, which create very strong intra- and intermolecular hydrogen bonds. This hydrogen-bond network renders cellulose hard to dissolve. Crystallinity in cellulose can be determined using X-ray diffraction,⁴ cross-polarization magic angle spinning nuclear magnetic resonance (CP-MAS NMR),⁵ and Fourier-transform infrared spectroscopy.⁶ The molecular weight of cellulose can be determined by end-group titration, osmometry, sedimentation velocity, capillary viscometer, light scattering or size exclusion chromatography (SEC), which is currently the method of choice.⁷ The average molecular weight is given either as number average molecular weight (M_n), z-average molecular weight (M_z), weight average molecular weight (M_w) or as viscosity average molecular weight (M_v).

Cellulose membranes (CMs) can be produced from cellulose type II, by regeneration from cellulose solution. CMs are frequently employed for separation in membrane technology due to their porous structure. The pore size and its distribution depend on the type of coagulant and coagulation parameters.⁸⁻¹⁰ Owing to their porous structure, CMs have the potential to be used as transparent and printable films by incorporation with polyvinyl alcohol.¹¹ The introduction of materials, such as graphene oxide (GO),¹² titanium dioxide (TiO₂)¹³ and bentonite¹⁴ particles, into the CM porous structure enhanced its permeability, electrical and antibacterial properties. The findings indicated that the introduction of GO and bentonite increased the pore size of the composites, while the incorporation of TiO₂ showed opposite results. First, CM with 0.005 wt% of GO exhibited a uniform pore size (0.9 nm), and consequently, led to high permeability (13.65 L m² h⁻¹) and low salt rejection (15.82%). Second, 6 wt% TiO₂-filled CM composite had the lowest pore size, ranging from 0.14 to 1 μm, and the highest zeta potential of 16.19 mV. The incorporation of 3% bentonite caused an increase in the interlayer distance to 1.71 nm with a tensile strength of 150 MPa.

In Malaysia, palm oil and kenaf are plant-based commodities with an estimated annual production of more than 5 MnT ha⁻¹ and 11 Tn ha⁻¹, respectively. Oil palm and kenaf plantations generate abundant wastes, such as oil palm empty fruit bunches (EFBs) and kenaf cores, respectively; these waste products are composed of approximately 34 to 37% cellulose.^{15,16} In this study, we investigated the chemical and physical properties of EFB and kenaf core pulps before proceeding with membrane preparation. The reason we used two types of pulps is to confirm and compare the pulp properties. This study focuses not only on utilizing waste biomass, but also on the development of value-added products.

EXPERIMENTAL

Materials

Oil palm EFB pulp sheets were purchased from Eko Pulp & Paper Sdn. Bhd., and kenaf core pulp was obtained from the Forest Research Institute Malaysia. The sodium chlorite (NaClO₂), glacial acetic acid (CH₃COOH), sodium hydroxide (NaOH), urea, 95-98% sulfuric acid, 37% hydrochloric acid (HCl), methanol (CH₃OH), ethanol (C₂H₅OH), *N,N*-dimethylacetamide (DMAc), 9*H*-fluoren-2-yl-diazomethane (FDAM) solution and lithium chloride (LiCl) pyridine, 4-dimethylaminopyridine, *N,O*-bistrifluoroacetamide, trimethylsilyl chloride and ethyl acetate employed in this study were of analytical grade, purchased from commercial sources and utilized as received.

Bleaching procedure

Oven-dried, disintegrated pulp was bleached *via* DEED treatment series, where D (first and fourth stages) comprised a chemical treatment with a mixture of 1.7% NaClO₂ and pH 4.5 buffer solution (a mixture of 27 g NaOH, 75 mL CH₃COOH, and 925 mL distilled water), and E was a treatment with 4% NaOH and 6% NaOH as the second and third stages, respectively. At every stage, the pulp was treated at 80 °C in a water bath for 2 h (D stage) and 1 h (E stage) and then washed with distilled water. The bleached pulp was oven-dried at 105 °C for 24 h before analysis.

Preparation of the membrane

NaOH/urea solvent was prepared by mixing 7 wt% NaOH: 12 wt% urea: 81 wt% distilled water and stored overnight in the freezer. The NaOH/urea solvent was removed and left at room temperature until the temperature reached -13 °C. 4 wt% of kenaf core and EFB pulps were dissolved in the NaOH/urea solvent and stirred at 2300 rpm using an overhead stirrer. The obtained cellulose solutions were centrifuged for 5 min at 10,000 rpm at 5 °C to separate the dissolved and undissolved parts of the cellulose solution. The dissolved cellulose was then used for membrane fabrication with two different thicknesses (0.04 mm and 0.07 mm) and was subsequently coagulated in 5% H₂SO₄. The membrane samples of 0.04 mm thickness and 0.07 mm thickness were denoted as CM0.04 and CM0.07, respectively. The undissolved part was disintegrated, washed repeatedly with distilled water until neutral, and dried at 80 °C for 24 h.

Monosaccharide analysis

The monosaccharide analyses of EFB and kenaf core pulps were conducted by immersing 2 mg of samples in 2 mL of 2 M acidic CH₃OH. The samples were agitated every 15 min to promote dissolution. After this, the samples were placed into an ultrasonic bath for 2 min and then were heated for 5 h in an oven (100 °C). Once the samples cooled, anhydrous pyridine and sorbitol standard solution were added. The mixture was agitated and evaporated in a N₂ environment. The samples were cooled to -80 °C and freeze-dried overnight before derivatization.

Derivatization was started with the addition of 200 μL anhydrous pyridine to the freeze-dried samples. After incubation at room temperature for 1 h, 4-dimethylaminopyridine and *N,O*-bistrifluoroacetamide (with 10% trimethylsilyl chloride) were added, and the samples were stored for 2 h at 70 $^{\circ}\text{C}$. Thereafter, 400 μL of ethyl acetate was added before analysis with GC-FID (Agilent Technologies Model 7890B). The injection volume was 1 μL at a split ratio of 10:1. An HP1 (Agilent 19091Z-413) methyl siloxane column (30 m \times 320 μm \times 0.25 μm) with H_2 as carrier gas at a flow rate of 2 mL min^{-1} was employed for the analysis. The oven temperature was set to 140 $^{\circ}\text{C}$ for 1 min, ramped at 4 $^{\circ}\text{C min}^{-1}$ to 210 $^{\circ}\text{C min}^{-1}$, and then heated at 30 $^{\circ}\text{C min}^{-1}$ to 260 $^{\circ}\text{C min}^{-1}$ with a holding time of 5 min. The temperatures of the injector and detector were retained at 260 $^{\circ}\text{C}$ and 280 $^{\circ}\text{C}$, respectively. The FID temperature was maintained at 320 $^{\circ}\text{C}$ with H_2 flow at 30 mL min^{-1} .

Crystallinity index

The solid-state NMR spectra of the wet pulps (~70 mg) were recorded on a Bruker Avance III HD 400 spectrometer (resonance frequency for ^1H 400.13 MHz and ^{13}C 100.61 MHz) equipped with a 4 mm dual-broadband CP-MAS probe. ^{13}C spectra were acquired using a total sideband suppression sequence at ambient temperature with a spinning rate of 5 kHz, cross-polarization (CP) contact time of 4 ms, recycle delay of 2 s, SPINAL-64 ^1H decoupling and acquisition time of 49 ms. The spectral width was set to 250 ppm. Chemical shifts were referenced externally against the carbonyl signal of glycine at $\delta = 176.03$ ppm. The crystallinity index (CrI) was determined as the integral ratio of the crystalline and amorphous region of C-4 based on Equation 1.¹⁷ The Dmfit program was employed to perform spectral fitting:¹⁸

$$\text{CrI (\%)} = \frac{A_{86-92 \text{ ppm}}}{A_{79-92 \text{ ppm}}} \times 100 \quad (1)$$

Molecular weight and carboxyl group determination

FDAM labelling, in combination with SEC, was applied to determine the molecular weight and carboxyl group content.¹⁹ For sample preparation, 20 mg of EFB and kenaf core pulps were suspended in 0.1 M HCl and disintegrated for 20 s in a blender. The pulps were washed with 0.1 M HCl, 96% $\text{C}_2\text{H}_5\text{OH}$ and DMAc before being filtered. For labelling, the pulp was suspended in 3 mL of DMAc and 1 mL of FDAM solution. The suspension was agitated in a water bath shaker at 40 $^{\circ}\text{C}$ for 7 days. Thereafter, the filtered reaction mixture was washed with DMAc and transferred to a dry vial. A total of 1.6 mL of DMAc/LiCl (9% m/v) was added to dissolve the cellulose. After it was dissolved, 0.3 mL of the sample was diluted with an additional 0.9 mL of DMAc, filtered through 0.45 μm filters, and measured using SEC.

The SEC system used in this study was equipped with a multiple-angle laser light scattering (MALLS), fluorescence detector (Shimadzu RF 535 [λ_{ex} : 280 nm; λ_{em} : 312 nm]) and a refractive index (RI) detector (Shodex RI-71). The SEC measurements were performed according to the following parameters: flow rate: 1.00 mL min^{-1} ; columns: four PL gel mixed ALS, 20 μm , 7.5 mm \times 300 mm; injection volume: 100 μL ; run time: 45 min; and mobile phase: 0.02 μm -filtered DMAc/LiCl (0.9% w/v). To determine the amount of dissolved material, an RI signal with a dn/dc of 0.136 mL g^{-1} and a detector constant of $5.32 \text{ E}^{-5} \text{ V}^{-1}$ were utilized. Data evaluation was performed with Astra 4.73, GRAMS/32 and Chromeleon software, while the molecular weight distribution (MWD) was replotted using Origin software.²⁰

Solubility test

The dissolution tests of EFB and kenaf core pulps were performed by immersing 4 wt% of pulp in 7 wt% NaOH, 12 wt% urea, and 81 wt% distilled water at -13 $^{\circ}\text{C}$. The pulps were stirred at 2300 rpm. The cellulose solution was centrifuged for 5 min at 10,000 rpm at 5 $^{\circ}\text{C}$ to separate the undissolved matter. The undissolved part was disintegrated, washed repeatedly with distilled water until neutral, dried at 80 $^{\circ}\text{C}$ for 24 h and weighed. The solubility was calculated using Equation 2:

$$\text{Solubility (S}_a\text{)} = \left(\frac{w_1 - w_2}{w_1} \right) \times 100 \quad (2)$$

where w_1 is the initial sample weight before dissolution, and w_2 is the weight of the dried insoluble residue.

Morphological analysis

The morphological analysis of the membranes was performed using a field emission-scanning electron microscope (FE-SEM Zeiss/Supra55VP) at an accelerating voltage of 3.0 kV. The membrane samples were freeze-dried before analysis. The images obtained by SEM were analysed to obtain the pore size distribution using ImageJ.

Transparency and tensile test

The transparency test was analysed using a JENWAY UV-vis 7315 spectrophotometer at a wavelength ranging from 200 to 800 nm under vacuum. The membrane samples were air-dried and cut to 1 cm \times 4 cm. The

tensile test of the membranes was carried out according to ASTM D882, using a tensile machine (GOTECH model AI-3000), with a 1 kg load, with a test speed of 5 mm min⁻¹, with a gauge length of 30 mm. The samples were air-dried for 24 h and cut into five pieces with dimensions of 6 cm × 1 cm.

RESULTS AND DISCUSSION

Monosaccharide composition

Table 1 shows the monosaccharide composition of EFB and kenaf core pulps. Although both types of pulps contained xylose and glucose, their concentrations were higher in EFB. Xylose is the main monosaccharide unit in xylan hemicellulose. This finding revealed that both pulps have xylan as a hemicellulose component.²¹ A small amount of mannose was detected only in EFB pulp (1.39 µg mg⁻¹); this result is consistent with previous findings.²² The remaining hemicellulose in the pulp was not completely removed from cellulose during pulping and bleaching, owing to the strong hydrogen bonding in the cellulose-hemicellulose system.²³ Glucose, another major monosaccharide, was detected in both pulps. This finding was attributed to the low molecular weight of the cellulose fractions, which had been degraded into glucose during analysis.²⁴

Crystallinity index

¹³C CP/MAS NMR spectroscopy was employed to determine the CrI of the two pulps. In general, crystalline cellulose I is a mixture of two distinct structures: triclinic cellulose I_α and monoclinic cellulose I_β. The influence of the magnetic field from the NMR instrument on the supramolecular structure of cellulose revealed well-resolved resonances for the crystalline and amorphous parts of C-4 and C-6 signals.²⁵ Based on previous literature, the C-4 and C-6 signals were suitable for crystallinity estimation for cellulose I, and cellulose II or mixtures of cellulose I and II, respectively.^{5,26} Figure 1 shows the CP-MAS ¹³C NMR spectra of EFB and kenaf core pulps. The peak at approximately δ 102-109 ppm was attributed to C-1, whereas the peak at approximately δ 80-91 ppm was attributed to the C-4 of cellulose. The signal from δ 69-79 ppm is composed of resonances from C-2, C-3 and C-5 and the signal from δ 59-67 ppm was assigned to C-6. Figure 2 (a) and (b) shows the spectral fitting of the C-4 region. Based on the manual deconvolution of the C-4 resonance, the CrI of 49.4% for EFB was slightly lower than the CrI of 51.5% for kenaf core pulp. The values from the peak fitting evaluation for EFB and kenaf core pulps were 48.8% and 51.8%, respectively, which are very close to the values gained from manual integration, where hemicellulose was considered.

Table 1
Monosaccharide contents detected in cellulose pulps

	EFB pulp (µg mg ⁻¹)	Kenaf core pulp (µg mg ⁻¹)
Glucose	53.62	46.12
Xylose	50.66	32.43
Mannose	1.39	—
Total	105.67	78.55

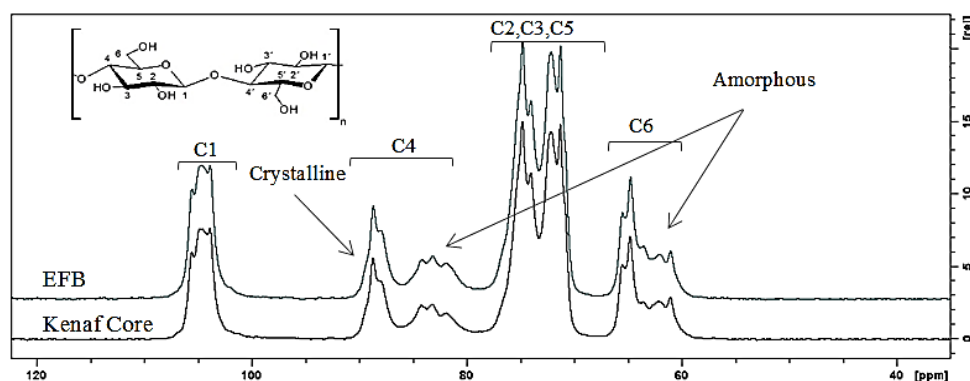


Figure 1: CP-MAS ¹³C NMR spectra of EFB and kenaf core pulps

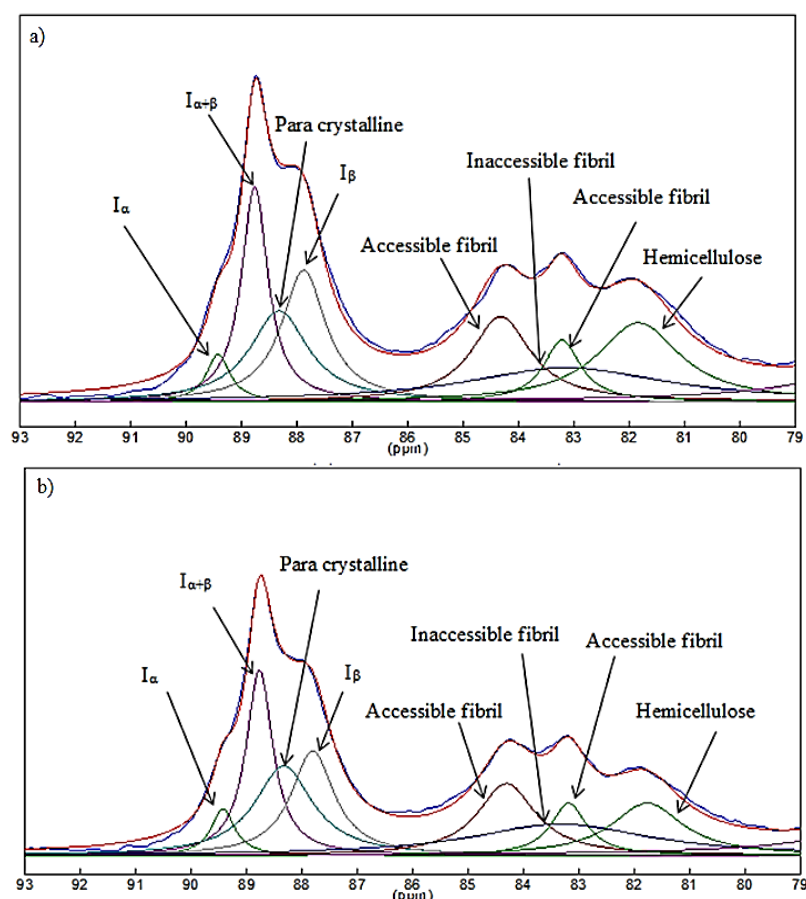


Figure 2: Spectral fitting (deconvolution) of the C-4 region in CP-MAS ^{13}C NMR spectra:
a) EFB pulp and b) kenaf core pulp

Table 2
Chemical shift regions used for spectral fitting of the C-4 region

	EFB bleached pulp			Kenaf core bleached pulp		
	δ (ppm)	Width (ppm)	Integral (%)	δ (ppm)	Width (ppm)	Integral (%)
I_α	89.43	0.51	3.1	89.43	0.51	3.6
$I_{\alpha+\beta}$	88.77	0.58	15.8	88.77	0.59	16.6
I_β	87.88	0.98	15.8	87.81	0.94	14.8
Paracrystalline	88.33	1.27	14.1	88.33	1.27	16.7
Accessible fibril surface	84.32	1.30	13.6	84.30	1.27	13.7
Accessible fibril surface	83.21	0.81	6.2	83.18	0.78	6.3
Inaccessible fibril surface	83.13	4.40	15.0	83.33	3.88	16.3
Hemicellulose	81.83	1.82	16.4	81.76	1.56	12.0

Table 2 shows the detailed assignment of the signals. The two I_α and I_β allomorphs provide two different ^{13}C shifts for C-4, according to the organization and orientation of the corresponding cellulose chain.²⁷ For both EFB and kenaf core pulp, I_α was detected at δ 89.43 ppm. However, I_β was detected at δ 87.88 ppm and 87.81 ppm for EFB core pulp and kenaf core pulp, respectively. I_β was more prominent than I_α in both EFB core pulp and kenaf core pulp. During the pulping process, chemicals and heat cause the unstable I_α to be converted to the more stable I_β .²⁸ Another four peaks were resolved via spectra fitting at the amorphous region of C-4 at approximately δ 81-84 ppm, which corresponds to accessible fibril surfaces, inaccessible fibril surfaces and hemicellulose.²⁹ From the integral percentage in Table 4, bleached kenaf pulps had higher amounts of accessible fibrils and inaccessible fibrils, which were 20% and 16.3%, respectively. According to previous work,³⁰ the surfaces of accessible fibrils easily get in contact with water, while inaccessible fibrils are water-inaccessible, formed because of interior distortion or aggregation of fibrils.³¹ Both accessible fibrils

and inaccessible fibrils were highly influenced by the dissolution of bleached pulps.³⁰ A hemicellulose signal was also obtained from these spectra fitting analyses. Hemicellulose detected in EFB bleached pulp (16.4%) was higher than that in kenaf bleached pulp (12%).

Molecular weight distribution and solubility

Figure 3 illustrates the MWD of EFB and kenaf core pulps. Both chromatograms show a monomodal cellulose peak, with a shoulder at approximately Log M_w 4.5 to Log M_w 5, originating from hemicelluloses or low-molecular-weight cellulose fractions, which have been identified in monosaccharide analysis. The weight average molecular weights (M_w) of EFB and kenaf core pulps were 4.76×10^5 g mol⁻¹ and 3.31×10^5 g mol⁻¹, respectively (Table 3). This result shows agreement with the trend observed by Baharin *et al.*,³² who reported that EFB pulp has a higher molecular weight than kenaf core pulp based on Ubbelohde viscometer measurements. The number average molecular weight (M_n) of EFB pulp (1.27×10^5) is higher than that of kenaf core pulp (1.07×10^5). EFB pulp showed a slightly higher dispersity ($\bar{D} = 3.78$), and consequently, provides a broader distribution than kenaf core pulp ($\bar{D} = 3.08$). As shown in Table 3, the amounts of carboxyl group content in EFB pulp and kenaf core pulp were of 20.67 $\mu\text{mol g}^{-1}$ and 30.86 $\mu\text{mol g}^{-1}$, respectively. The difference in carboxyl group amounts was due to the variation in biomass and its purity. Each biomass contains different amounts of hemicellulose, which is a major contributor to the amounts of carboxyl groups in the form of uronic acid moieties.^{33,34} However, these amounts reflect a higher number of hemicellulose and are associated with the oxidation of C-6 hydroxyl. During bleaching, the hydroxyl groups at C-6 of cellulose were converted to carboxylic acids.³⁵ Because of the variation in biomass, EFB and kenaf core pulps behaved differently during the bleaching process, which consequently led to different amounts of the carboxyl group. The carboxyl group is very sensitive and tends to degrade in an alkaline environment, which consequently affects the dissolving process of pulp and the formation of CM.³⁶

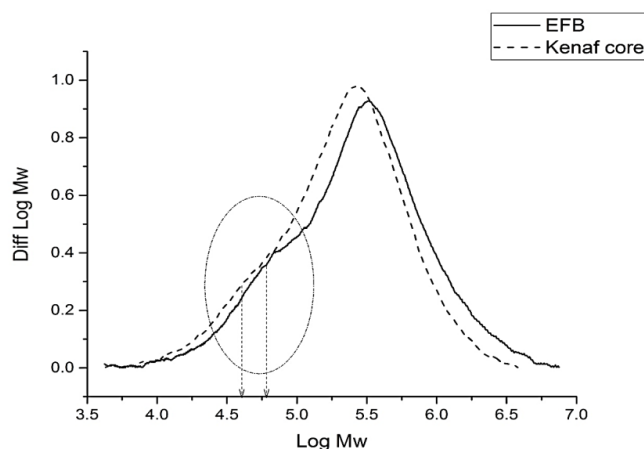


Figure 3: Molecular weight distribution of cellulose pulps from kenaf core and EFB; the shoulder at approximately Log M_w 4.5 to Log M_w 5 arises from hemicellulose or low-molecular-weight cellulose fractions

Table 3
Molecular weight distribution of EFB and kenaf core pulps

Pulp	M_w (g mol ⁻¹)	M_n (g mol ⁻¹)	Dispersity \bar{D}	Carboxyl group content ($\mu\text{mol g}^{-1}$)
EFB	4.76×10^5	1.27×10^5	3.73	20.67
Kenaf core	3.31×10^5	1.07×10^5	3.08	30.86

Table 4
Weight percentages of cellulosic pulps in different molecular weight regions

DP	Kenaf core (%)	EFB (%)
<100	1.51	1.08
100-200	4.34	3.10
200-2000	59.83	51.45
>2000	34.3	44.35

Table 5
Solubility of cellulosic pulps in NaOH/urea solvent

Pulp	Solubility (%)
Kenaf core	73.10 ± 0.13
EFB	32.95 ± 0.52

Table 4 shows the percentage contents of four different molecular weight regions (degree of polymerization (DP) ranges), which are often utilized to describe the differences in the cellulosic pulps. The DP represents the number of AGUs in a cellulose chain. The DP was obtained by splitting the MWD at the respective DP range and auto-calculated using software. The DP values of the EFB pulp and the kenaf core pulp, which are below 200, were 4.18% and 5.85%, respectively. This result represented a mixture of hemicellulose and low-molecular-weight cellulose.³⁷⁻³⁹ The kenaf core pulp consists of a higher DP of 200-2000, with almost 60% compared with the EFB pulp, which is only 51%. However, EFB pulps exhibit a 10% higher DP value of >2000 than the kenaf core pulp, which shows that EFB has not only a higher M_w , but also a higher DP than kenaf core pulp. During bleaching, cellulose tends to slightly depolymerize because of the utilization of sodium chlorite and acetic acid in the bleaching procedure.⁴⁰ Kenaf pulp is extensively degraded after it is bleached, compared with EFB pulp.³² This finding suggests that EFB pulp can be restrained from severe depolymerization due to a high DP. The difference in plant species may be another factor influencing the different weight percentages in the respective regions.⁴¹

Cellulose hardly dissolves in water and most organic solvents. However, the solubility data (Table 5) shows that the solubility of EFB and kenaf core pulps, with 33% and 73%, respectively, in NaOH/urea is possible. This solubility occurred due to (i) the breakdown of intermolecular hydrogens at low temperature (<10 °C), (ii) NaOH hydration and interaction with cellulose, and (iii) urea hydration prevented agglomeration of cellulose.⁴² Kenaf was accessible to dissolve in NaOH/urea due to its high content of carboxyl group, and hence, enhanced the swelling of cellulose. Nonetheless, EFB pulp showed lower solubility than kenaf core pulp, because of its higher molecular weight and DP.

Morphological analysis

Membranes with two thicknesses (0.04 mm and 0.07 mm) were prepared to determine the effect of thickness on the morphological properties. Figure 4 (a and b) shows the cross-section morphology of CM0.04 and CM0.07 prepared from kenaf core bleached pulp. The morphological analysis of the EFB membrane is not shown because it was not successfully formed because of the solubility limitation. Both cross-section images showed inhomogeneous pore distribution. From ImageJ, the pore size for CM0.07 ranges from 1 to 2000 μm , while the pore size of CM0.04 mm ranges from 1 to 6500 μm . The use of H_2SO_4 produced a membrane with small pore sizes.⁴³ However, in the present study, this result was due to the longer coagulation time. CM0.07 was detached from the glass slide after 15 min, while CM0.04 was detached from the glass slide after 5 min. This difference allowed greater reformation of new hydrogen bonding among cellulose molecules in CM0.07 during the coagulation process,^{11,44} and a CM with small pores was formed.

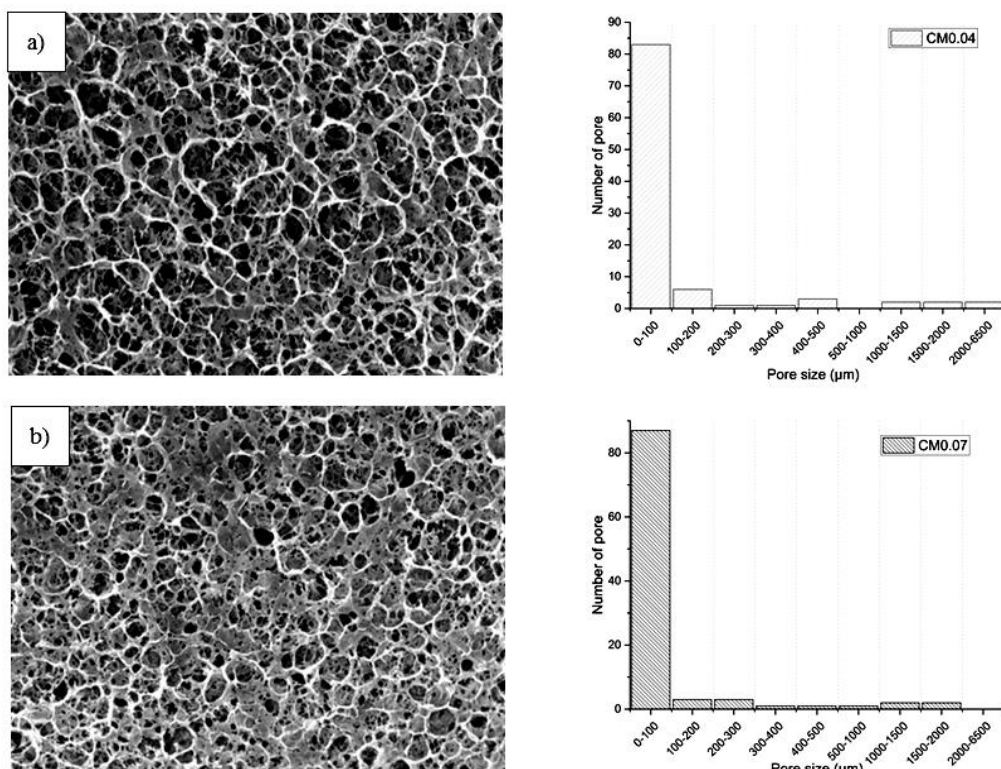


Figure 4: Distribution of pores of a) CM0.04 and b) CM0.07 – significantly affected by membrane thickness

Table 6
Tensile and transparency properties of CM at two different thicknesses

Properties	CM0.04	CM0.07
Tensile strength (MPa)	23.78	33.48
Maximum load (N)	10.18	25.55
Elongation (%)	6.50	8.03
Young's modulus, E (MPa)	1288.38	2138.52
Transparency (%)	44.48	20.54

Tensile and transparency test

Table 6 shows the tensile and transparency properties of CM0.04 and CM0.07. The tensile properties of CM0.07 were higher than those of CM0.04. CM0.07 had a tensile strength of 33.48 MPa, with a maximum load of 25.55 N and 8% elongation. The excellent tensile properties of CM0.07 were due to its smaller pore size and rigid structure.⁴⁵ In addition, the tensile properties could also be due to the presence of the hemicellulose that remained and was entangled in the pulp. Hemicellulose promotes cellulose alignment and acts as a plasticizer, which consequently enhanced the mechanical properties of the CM.⁴⁶ However, the presence of the hemicellulose membrane and low pore sizes caused the scattering of the incident light, which weakened the membrane and led to low transparency for CM0.07 (20.54%).⁴⁷

CONCLUSION

In this study, we discovered that kenaf core and EFB bleached pulps behaved differently in the same bleaching procedure. The low molecular weight and DP, as well as the high accessibility of fibril surfaces and carboxyl group of kenaf core bleached pulp allowed the production of membranes with reasonable mechanical properties. EFB had a longer polymer chain, which limited dissolution and membrane formation. The membrane thickness had a crucial effect on the membrane properties, such as tensile strength and transparency. The CM0.07 membrane had a smaller pore size than CM0.04, which enhanced the tensile properties and reduced the transparency of the membrane.

ACKNOWLEDGEMENTS: The authors would like to acknowledge the financial support of the Malaysian Ministry of Higher Education via FRGS/1/2018/STG07/UKM/01/1, DIP-2018-033, Erasmus Mundus ALFABET for supporting the mobility at Christian-Doppler Laboratory of the University of Natural Resources and Life Sciences (BOKU), Vienna, and MyBrain15.

REFERENCES

- ¹ B. Norizan, N. U. R. Sauta, S. N. A. Syed Hashim, S. Zakaria, M. Daud *et al.*, *Cellulose Chem. Technol.*, **53**, 1001 (2019), <https://doi.org/10.35812/CelluloseChemTechnol.2019.53.98>
- ² J. Gominho, A. Lourenço, D. Neiva, L. Fernandes, M. Amaral *et al.*, *Eur. J. Wood Wood Prod.*, **74**, 101 (2016), <https://doi.org/10.1007/s00107-015-0965-2>
- ³ M. S. Jahan, S. Rawsan, D. A. Nasima Chowdhury and A. Al-Maruf, *BioResources*, **3**, 1359 (2008), https://ojs.cnr.ncsu.edu/index.php/BioRes/article/view/BioRes_03_4_1359_Jahan_RNA_Atl_Pulping_Dissolv_Jute
- ⁴ E. Hafemann, R. Battisti, D. Bresolin, C. Marangoni and R. A. F. Machado, *Waste Biomass Valorif.*, (2020), <https://doi.org/10.1007/s12649-020-00937-2>
- ⁵ X. Zhu, Y. Dai, C. Wang and L. Tan, *Contributions to Tobacco Research*, **27**, 126 (2016), <https://doi.org/10.1515/cttr-2016-0014>
- ⁶ N. Kruer-Zerhusen, B. Cantero-Tubilla and D. B. Wilson, *Cellulose*, **25**, 37 (2018), <https://doi.org/10.1007/s10570-017-1542-0>
- ⁷ A. Potthast, S. Radosta, B. Saake, S. Lebioda, T. Heinze *et al.*, *Cellulose*, **22**, 1591 (2015), <https://doi.org/10.1007/s10570-015-0586-2>
- ⁸ J. Cai, L. Wang and L. Zhang, *Cellulose*, **14**, 205 (2007), <https://doi.org/10.1007/s10570-007-9106-3>
- ⁹ N. A. Azahari, S. Gan, S. Zakaria, H. Kaco and S. Moosavi, *Cellulose Chem. Technol.*, **52**, 201 (2018), [http://www.cellulosechemtechnol.ro/pdf/CCT3-4\(2018\)/p.201-207.pdf](http://www.cellulosechemtechnol.ro/pdf/CCT3-4(2018)/p.201-207.pdf)
- ¹⁰ N. S. N. Mazlan, S. Zakaria, S. Gan, C. C. Hua and K. W. Baharin, *CERNE*, **25**, 18 (2019), <http://dx.doi.org/10.1590/01047760201925012586>
- ¹¹ H. Kaco, S. Zakaria, C. H. Chia and L. Zhang, *BioResources*, **9**, 2167 (2014), <https://doi.org/10.15376/biores.9.2.2167-2178>
- ¹² F. Khili, J. Borges, P. L. Almeida, R. Boukherroub and A. D. Omrani, *Waste Biomass Valorif.*, **10**, 1913 (2019), <https://doi.org/10.1007/s12649-018-0202-4>
- ¹³ C. Das and K. A. Gebru, *Journal of The Institution of Engineers (India): Series E*, **98**, 91 (2017), <https://doi.org/10.1007/s40034-017-0104-1>
- ¹⁴ O. V. Alekseeva, A. N. Rodionova, N. A. Bagrovskaya, A. V. Agafonov and A. V. Noskov, *Arabian J. Chem.*, **12**, 398 (2019), <https://doi.org/10.1016/j.arabjc.2015.07.011>
- ¹⁵ Y. C. Ching and T. C. Ng, *BioResources*, **9**, 6373 (2014), https://ojs.cnr.ncsu.edu/index.php/BioRes/article/view/BioRes09_4_6373_Ching_Cellulose_Oil_Palm_Fiber
- ¹⁶ I. Kamal, M. Z. Thirmizir, G. Beyer, M. J. Saad, N. A. A. Rashid *et al.*, *J. Sci. Technol.*, **6**, 41 (2014), <https://publisher.uthm.edu.my/ojs/index.php/JST/article/view/796>
- ¹⁷ R. H. Newman, *Holzforschung*, **58**, 91 (2004), <https://doi.org/10.1515/HF.2004.012>
- ¹⁸ D. Massiot, F. Fayon, M. Capron, I. King, S. L. Calvé *et al.*, *Magn. Resonan. Chem.*, **40**, 70 (2002), <https://doi.org/10.1002/mrc.984>
- ¹⁹ J. Röhring, A. Potthast, T. Rosenau, T. Lange, G. Ebner *et al.*, *Biomacromolecules*, **3**, 959 (2002), <https://doi.org/10.1021/bm020029q>
- ²⁰ A. Potthast, T. Rosenau, P. Kosma, A.-M. Saariaho and T. Vuorinen, *Cellulose*, **12**, 43 (2005), <https://doi.org/10.1023/B:CELL.0000049347.01147.3d>
- ²¹ T. Y. Ying, L. K. Teong, W. N. W. Abdullah and L. C. Peng, *Procedia Environ. Sci.*, **20**, 328 (2014), <https://doi.org/10.1016/j.proenv.2014.03.041>
- ²² R. Ibrahim, *Oil Palm Bull.*, **44**, 19 (2002), <https://www.cabdirect.org/cabdirect/abstract/20023162448>
- ²³ X. Zhang, W. Yang and W. Blasiak, *Energ. Fuels*, **25**, 4786 (2011), <https://doi.org/10.1021/ef201097d>
- ²⁴ F. Zeinaly, A. Saraeian, K. Gabov and P. Fardim, *Cellulose Chem. Technol.*, **51**, 45 (2017), [http://www.cellulosechemtechnol.ro/pdf/CCT1-2\(2017\)/p.45-53.pdf](http://www.cellulosechemtechnol.ro/pdf/CCT1-2(2017)/p.45-53.pdf)
- ²⁵ G. Zuckerstätter, G. Schild, P. Wollboldt, T. Röder, H. Weber *et al.*, *Lenzinger Berichte*, **87**, 38 (2009), <https://www.semanticscholar.org/paper/The-elucidation-of-cellulose-supramolecular-by-13CZuckerstaetterSchild/c27d9881db5e023aba0bbc3ae76f22e158863349>
- ²⁶ A. Mittal, R. Katahira, M. E. Himmel and D. K. Johnson, *Biotechnol. Biofuels*, **4**, 1 (2011), <https://doi.org/10.1186/1754-6834-4-41>
- ²⁷ H. Kono and Y. Numata, *Cellulose*, **13**, 317 (2006), <https://doi.org/10.1007/s10570-005-9025-0>
- ²⁸ S. Maunu, T. Liitiä, S. Kauliomäki, B. Hortling and J. Sundquist, *Cellulose*, **7**, 147 (2000), <https://doi.org/10.1023/A:1009200609482>

- ²⁹ K. Wickholm, P. T. Larsson and T. Iversen, *Carbohydr. Res.*, **312**, 123 (1998), [https://doi.org/10.1016/S0008-6215\(98\)00236-5](https://doi.org/10.1016/S0008-6215(98)00236-5)
- ³⁰ V. Chunilall, T. Bush and P. T. Larsson, in “Fundamental Aspects”, edited by T. V. D. Ven and L. Godbout, IntechOpen, 2013, pp. 69-90, <https://www.intechopen.com/books/cellulose-fundamental-aspects>
- ³¹ E. L. Hult, P. T. Larsson and T. Iversen, *Polymer*, **42**, 3309 (2001), [https://doi.org/10.1016/S0032-3861\(00\)00774-6](https://doi.org/10.1016/S0032-3861(00)00774-6)
- ³² K. W. Baharin, S. Zakaria, A. V. Ellis, N. Talip, H. Kaco *et al.*, *Sains Malaysiana*, **47**, 377 (2018), [http://www.ukm.my/jsm/pdf_files/SM-PDF-47-2-2018/UKM%20SAINSMalaysiana%2047\(02\)Feb%202018%2020.pdf](http://www.ukm.my/jsm/pdf_files/SM-PDF-47-2-2018/UKM%20SAINSMalaysiana%2047(02)Feb%202018%2020.pdf)
- ³³ W. Judiawan, Y. Sudiyani and E. Nurnasari, *Indonesian J. Appl. Chem.*, **21**, 14 (2019), <https://doi.org/10.14203/jkti.v21i1.412>
- ³⁴ S. Palamae, P. Dechatiwongse, W. Choorit, Y. Chisti and P. Prasertsan, *Carbohydr. Polym.*, **155**, 491 (2017), <https://doi.org/10.1016/j.carbpol.2016.09.004>
- ³⁵ L. C. A. Barbosa, C. R. A. Maltha, A. J. Demuner, C. M. Cazal, E. L. Reis *et al.*, *Bioresources*, **8**, 1043 (2013), https://ojs.cnr.ncsu.edu/index.php/BioRes/article/view/BioRes_08_1_1043_Barbosa_Quantification_Carboxyl_Groups
- ³⁶ J. Perrin, F. Pouyet, C. Chirat and D. Lachenal, *Bioresources*, **9**, 7299 (2014), http://stargate.cnr.ncsu.edu/index.php/BioRes/article/view/BioRes_09_4_7299_Perrin_Carbonyl_Carboxyl_Groups_Cellulosic_Pulps
- ³⁷ T. A. Gulbrandsen, I. A. Johnsen, M. T. Opedal, K. Toven, K. Øyaas *et al.*, *Cellulose Chem. Technol.*, **49**, 117 (2015), [http://www.cellulosechemtechnol.ro/pdf/CCT2\(2015\)/p.117-126.pdf](http://www.cellulosechemtechnol.ro/pdf/CCT2(2015)/p.117-126.pdf)
- ³⁸ J. Röhring, A. Potthast, T. Rosenau, T. Lange, A. Borgards *et al.*, *Biomacromolecules*, **3**, 969 (2002), <https://doi.org/10.1021/bm020030p>
- ³⁹ A. Potthast, J. Röhring, T. Rosenau, A. Borgards, H. Sixta *et al.*, *Biomacromolecules*, **4**, 743 (2003), <https://doi.org/10.1021/bm025759c>
- ⁴⁰ C. A. Hubbell and A. J. Ragauskas, *Bioresour. Technol.*, **101**, 7410 (2010), <https://doi.org/10.1016/j.biortech.2010.04.029>
- ⁴¹ G. Siqueira, J. Bras and A. Dufresne, *Polymers*, **2**, 728 (2010), <https://doi.org/10.3390/polym2040728>
- ⁴² M. G. Walters, A. D. Mando, W. Matthew Reichert, C. W. West, K. N. West *et al.*, *RSC Adv.*, **10**, 5919 (2020), <https://doi.org/10.1039/c9ra07989k>
- ⁴³ L. Zhang, Y. Mao, J. Zhou and J. Cai, *Ind. Eng. Chem. Res.*, **44**, 522 (2005), <https://doi.org/10.1021/ie0491802>
- ⁴⁴ S. Zhang, F. X. Li and J. Y. Yu, *Cellulose Chem. Technol.*, **45**, 593 (2010), [http://www.cellulosechemtechnol.ro/pdf/CCT45,9-10\(2011\)/p.593-604.pdf](http://www.cellulosechemtechnol.ro/pdf/CCT45,9-10(2011)/p.593-604.pdf)
- ⁴⁵ N. A. Azahari, S. Gan, S. Zakaria, H. Kaco and S. Moosavi, *Cellulose Chem. Technol.*, **52**, 201 (2018), [http://cellulosechemtechnol.ro/pdf/CCT3-4\(2018\)/p.201-207.pdf](http://cellulosechemtechnol.ro/pdf/CCT3-4(2018)/p.201-207.pdf)
- ⁴⁶ J. H. Chen, Y. Guan, K. Wang, F. Xu and R. C. Sun, *Cellulose*, **22**, 1505 (2015), <https://doi.org/10.1007/s10570-015-0608-0>
- ⁴⁷ Y. Wang, L. Yuan, H. Tian, L. Zhang and A. Lu, *J. Membrane Sci.*, **585**, 99 (2019), <https://doi.org/10.1016/j.memsci.2019.04.059>